Exploring theoretical limits of statistical room acoustics

Andor T. Fürjes[1]

[1]*aQrate Acoustics Ltd.*

This contribution has been accepted based on the submitted abstract. The submitted manuscript was not reviewed and is reproduced here without edits or corrections by the conference board. Neither the EAA nor the AAA take responsibility for its contents.

Preliminary document

Abstract

Applicability of statistical room acoustic equations is a core issue in acoustic engineering practice and traditionally assumes a diffuse sound field and a non-modal frequency range by theory. Ideal conditions are hard to meet in practice, but still, these equations are used and are working satisfactorily in most cases. In order to find and quantify limiting cases of size, proportion, non-uniform absorption etc., the paper discusses results of numerical experiments based on the mirror image source model of rectangular rooms.

Keywords: room acoustics, limits of statistical approximation, non-diffuse sound fields, non-uniform absorption, normalized mean free path length, spatial variability

1. Introduction

Acoustic engineers have access to sophisticated room acoustic modelling tools now, but for practical reasons use or at least start the work with simple equations based on statistical assumptions (SA) in most cases.

In room acoustics, the most known condition of applicability of simple equations is the existence of a diffuse sound field.

In the frequency domain the Schroeder-frequency [1] (SF) is used to indicate a lower limit for stochastic behavior. Here the condition is, that adjacent modes cannot act independently from another above the cutoff or cross-over frequency:

$$f_{Sch} = k/k_0 \cdot (T_{60}/V)^{1/2} \quad (1)$$

where T_{60} is the 60 dB decay time at the frequency of interest, V is the cubic volume of the room, $k_0 = 1(s/m)^{3/2}$ and k is a constant.

Usually, $k = 2000$ is used, derived from the condition of 3-fold overlapping of modes, but values between 900 and 4000 can be considered as well (see [2]).

The formula assumes that each mode is equally important in spreading energy, which might not be correct when spatial distribution of absorption is not uniform. Experimentally the cutoff frequency cannot be observed directly, because the transition from 'modal' and 'non-modal' frequency regimes is not abrupt. Correlations to descriptors like e.g. critical distance (see [3]) is somewhat self-explanatory, since they use the same T_{60}/V ratio.

The other usual condition is to find a time limit, a so-called 'mixing time' from where the response shows dominant stochastic properties (e.g. [4]) or echo density is high enough (e.g. [5]).

Existence and quality of a diffuse sound field can be expressed in many ways (e.g. [6]) and when assuming the validity of SA in room acoustics, tremendous theoretical and experimental work has been done (e.g. [7]), yet easily applicable indicators for engineering practice are not explored beyond the ones above.

For the cases of rooms with rectangular shape, the mirror image source model (MISM, see e.g. [8]) is the most practical approach for wide frequency range, when assuming uniform sound absorption within each boundary. When admittance is known, angle-dependent reflections can be considered (see [9]), but diffuse reflections are not covered by the model.

This paper explores new practical indicators based on MISM results, in order to check if theoretical pre-conditions of SA can be met and how these are affected by usual attributes like room proportions or non-uniform sound absorption. Section 2 outlines main assumptions and the scope. Section 3 discusses the concept of mean free path length (MFPL) in the context of a MISM. Section 4 calculates development of isotropy in a MISM and how room proportions affect this development. Section 5 and 6 discuss consequences of a non-uniform sound absorption on the development of isotropy and spatial decay of reverberant sound levels. Section 7 shows the observation, that normalized standard deviation (nSD) could be an indication on the uniformity of room response to pure tone excitation. Section 8 gives a summary of the results.

2. Hypothesis

A simple statistical model of a complex dynamic system can be valid, if the system consists of a large number of independent stable processes which behave similarly and dissimilar processes are negligible in the whole set (conditions of ergodicity and statistical stability).

In room acoustics, there are infinite processes, which are stable due to the lossy nature of sound reflection

and propagation. Statistical similarity of these processes can be assumed for convex rooms (where mutual visibility of boundary surface elements is high), but still requires isotropy. Therefore, isotropy is a necessary condition for a simple statistical description. On the other hand, homogeneity is not a necessary but a sufficient condition, because homogeneity by itself is the proof of statistical similarity.
Quality of isotropy and homogeneity are not constant, but change (assumingly increase) with time within the response.
Statistical similarity will end up taking the form in the response as a sum of exponential decays. Practical approaches in the engineering sense approximate the combined, dominant exponential energetic decay of the response, which is governed by a temporal inertia τ and damping B:

$$E(t) = A \cdot B^{-t/\tau}, \tag{2a}$$

and amplitude A is not relevant in calculating the time required to reach -60 dB decay level

$$T_{60} = 6 \cdot ln(10) \cdot \tau/B. \tag{2b}$$

This scheme is clearly recognizable in papers summarizing usual reverberation time formulas (e.g. [10]). For example, to get reverberation time $T_{60,E}$ according to the Eyring-formula, one must apply $\tau = l_{mfpl}/c$ with MFPL in l_{mfpl} and speed of wave propagation in c, while $B = m \cdot l_{mfpl} - ln(1 - \bar{\alpha}_s)$ with absorption of air in m of air in 1/m unit and mean absorption of surfaces in $\bar{\alpha}_s$.
The intrinsic question is then, how development of isotropy and homogeneity is affected by attributes like size and shape of the room, quantity and distribution of absorption, irregularities of surfaces (diffusity) in the room and how these will affect τ/B ratio in (2b) in simple terms.
During discussion of the results, variability of a dataset is qualified by the normalized standard deviation $nSD = SD/RMS$, which conveniently has a $0 \ldots 1$ range. A result of 1 means high variability (no bias) in the set, while 0 means no variability (but bias). Value sets with near 0 mean value, e.g. full periods of sinusoidal signals or $sinc(x)$ functions beyond $x = 0 \ldots > 9\pi$ interval) will have a $nSD > 0.99$ value.

3. Mean free path length in a specular model

Isotropy in a MISM means, that image sources along a thin temporal spherical shell appear uniformly distributed (i.e. energy density of image sources is uniform within thin spherical shells). This implies, that a MFPL can be derived, considering image sources in all directions represent paths that have gone thru more or less the same number of reflections.
For example, along the z axis, the average number of reflections is $n_z = (r/2)/H$, because $r/2$ is the average height of a sphere with radius r.
The total number of reflections n_{xyz} must include the x and y axis as well, hence

$$n_{xyz} = n_x + n_y + n_z = \frac{c \cdot t/2}{L} + \frac{c \cdot t/2}{W} + \frac{c \cdot t/2}{H}. \tag{3a}$$

The average path length is the total path length $r = c \cdot t$ divided by the total number of reflections:

$$l_{mfp} = \frac{c \cdot t}{n_{xyz}} = \frac{2}{\frac{1}{L}+\frac{1}{W}+\frac{1}{H}} = \frac{4V}{S} \tag{3b}$$

which is the same, as the MFPL derived traditionally from classic diffuse field theory (e.g. [11]).
Similarly, 2D isotropy e.g. in the xy plane (along L and W dimensions) can lead to the concept of a 2D MFPL. The average height $r \cdot 2/\pi$ of a semicircle gives

$$l_{mfp,xy} = \frac{c \cdot t}{n_x + n_y} = \frac{c \cdot t}{\frac{c \cdot t \cdot 2/\pi}{L} + \frac{c \cdot t \cdot 2/\pi}{W}} = \frac{\pi}{2} \frac{L \cdot W}{L + W} \tag{4}$$

as the mean free path in a 2D scene. This will then give the same results as known for 2D approximated situations (see e.g. [12]).

4. Isotropy in a specular model

Isotropy of reflections can be measured directly in a MISM by summing reflection intensities thru faces of a regularly tiled sphere (Figure 1). In this example, each face of a polyhedron (5,3,2) centered at the receiver position represents a direction and a $4\pi/120$ solid angle.

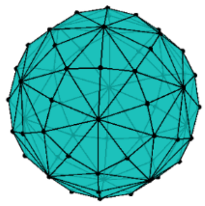

Figure 1. A polyhedron (5,3,2) with 120 uniform triangular faces used to detect directional distributions.

Directional probability of the response for time intervals and nSD of probability is calculated (see Figure 2). Visually, directional distribution seems uniform pretty soon, already by about $150 \cdot l_{mfp}$.

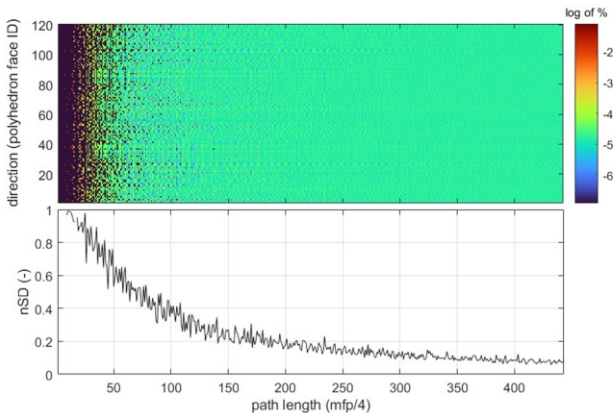

Figure 2. Directional probability (top) and nSD of probability of the response from image sources (room L:W:H = 1:1:1), considering 120 directions and $\Delta t = l_{mfp}/(4 \cdot c)$ intervals.

Corresponding author: *furjes.andor@aqrate.hu*
Copyright: *©2026 Andor T. Fürjes. This is an open-access article distributed under the terms of the Creative Commons Attribution 3.0 Unported License, which permits unrestricted use, distribution, and reproduction in any medium, provided the original author and source are credited.*

Preliminary document

A lower nSD value means less directional variability, hence a higher isotropy. Using this approach, temporal development of isotropy for different room proportions can be compared (Figure 3). In this numerical experiment, models of 100 m^3 rectangular rooms with different proportions and uniform absorptions are used with up to 1 s radius ($N \approx 1.7 \cdot 10^6$ images).

As expected, time required to reach a chosen lower threshold of nSD correlates with dimensional proportions of the room. Figure 4 shows two candidates to embody this observation. Of different candidates tried, form factor $l_n = l_{mfp}/\sqrt{S}$ (suggested in [13]) has a very strong correlation with this rate of change.

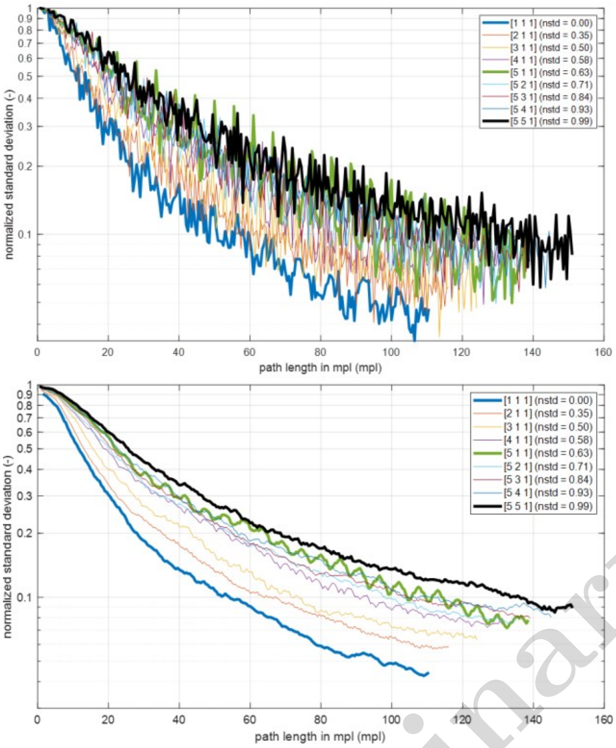

Figure 3. Directional variability vs. time in response (top: for each bin, bottom: $4 \cdot l_{mpl}$ moving average smoothing for a clearer comparison).

Based on these tendencies, a temporal indicator of isotropy ($nSD < 0.1$) in a purely specular field can be:

$$t_{iso} \approx (-700 \cdot l_n + 244) \cdot l_{mfp}/c \qquad (5)$$

In this example, the threshold of $nSD < 0.1$ is arbitrarily chosen and can be revised later.

Please note, that this experiment did consider only uniform sound absorption and did not consider any scattering (which would accelerate isotropy). Also, even if a 1:1:1 room ratio shows the best chance of becoming isotropic soon, it does not mean it has preferable qualities over other room proportions.

5. Non-uniform sound absorption

In an isotropic state, image sources with similar energies and reflection order are supposed to be found in concentric spherical shells around the original source. When boundaries have different sound absorptions, this spherical symmetry will be distorted ("squeezed") along directions, where absorption is higher and form a triaxial ellipsoid. This distortion might be compensated ("de-squeezed") by assuming that the new spatial distribution can be equivalent to a room with uniform sound absorption but different ("apparent") sizes (Figure 5).

The compensation is based on the idea, that if in 1D setup sound absorption is changed from α_L to α_L', the power level of images along L grid at distance $r = c \cdot t$ are the same, when changing the characteristic length from L to L' accordingly based on the equation

$$(1-\alpha_L)^{r/L} = (1-\alpha_L')^{r/L'} \qquad (6a)$$

or

$$(\beta_L)^{r/L} = (\beta_L')^{r/L'} \qquad (6b)$$

hence

$$L' = L \cdot log(\beta_L')/log(\beta_L) \qquad (6c).$$

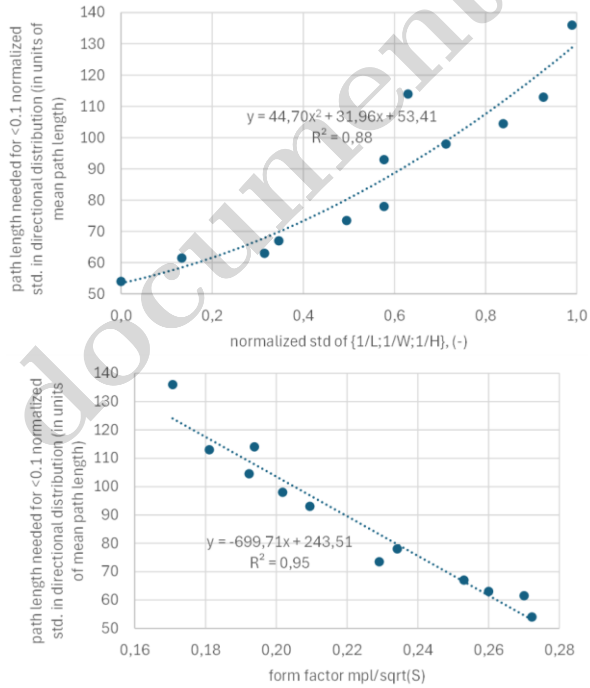

Figure 4. Correlation of minimum path length to reach $nSD < 1$ of directional variability as a function of shape: $nSD\{L^{-1};W^{-1};H^{-1}\}$ (top), $l_n = l_{mpl}/\sqrt{S}$ (bottom).

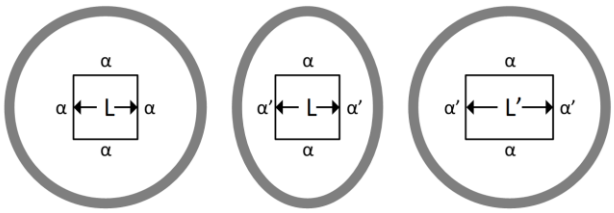

Figure 5. Explanation of apparent size to correct spatial imbalance of image source energies: uniform absorption α featuring spherical isotropy (left), non-uniform absorption $\alpha' > \alpha$ featuring ellipsoid isotropy (center), corrected apparent size L' to yield spherical isotropy with non-uniform absorption α' (right).

In a 3D setup, a common reference β_O shall be the maximum of combined reflected energies for each direction, because any lower reflectance will change the spherical symmetry of energy distribution. Combined

Preliminary document

reflectance along direction L is $\beta_L = \beta_{L,0} \cdot \beta_{L,1}$, where $\beta_{L,0} = 1 - \alpha_{L,0}$ and $\beta_{L,1} = 1 - \alpha_{L,1}$ are reflections from rear and front respectively.
The same can be applied to include width and height:

$$\begin{bmatrix} L' \\ W' \\ H' \end{bmatrix} = \begin{bmatrix} L \\ W \\ H \end{bmatrix} \begin{bmatrix} log(\beta_L) \\ log(\beta_W) \\ log(\beta_H) \end{bmatrix} \Big/ log(\beta_O) \qquad (7a)$$

where $\beta_O = max\{\beta_L; \beta_W; \beta_H\}$. Then from (3b)

$$l'_{mfp} = 2/(1/L' + 1/W' + 1/H') \qquad (7b)$$

gives an 'apparent' MFPL and a form factor

$$l'_n = l'_{mfp}/\sqrt{S'} = \mu \cdot l_n. \qquad (7c)$$

where $\mu \geq 1$ represents the change due to non-uniform sound absorption.
For example, let us have a room with 9×6×3 m dimensions and $\alpha = 0.10$ absorption on all its surfaces, where $l_n = 0.23$ and $t_{iso} = 0.77s$. Because t_{iso} is smaller than $T_{60,E} = 1.25s$, the classic formula should be valid. However, when increasing ceiling absorption to $\alpha'_{H,1} = 0.90$, the values change to $l'_n = 0.19$ and $t'_{iso} = 1.04s$. Now t'_{iso} is significantly higher than $T'_{60,E} = 0.34s$, which indicates the classic formula is probably not valid. This fits expectations, as a room with highly absorbing ceiling, non-absorbing walls and without diffusing elements is known to behave oddly.
According to (2b) it is possible to give a new reverberation time formula for empty rectangular rooms with barely scattering walls based on l'_{mfp} as

$$T^{\square}_{60,M} = \frac{6 \cdot ln(10)}{c} \frac{l'_{mfp}}{m \cdot l^{\square}_{mfp} - ln(1-\bar{\alpha}_s)} = \mu \cdot T_{60,E} \qquad (8)$$

with the concept, that non-uniform sound absorption will multiply inertia τ by factor $\mu \geq 1$, but not the damping B in (2b). Testing this formula will be a topic of another investigation.

6. Spatial decay of sound levels

In contrast to classic room acoustic theory, observed reverberant sound levels are not uniform, but decrease with distance from the source [14]. The rate of spatial decay can be rewritten using the MFPL [15] as if spherical symmetry of image sources can be extended back to the original source (see Figure 6). With slight modifications [13] the total sound level is then expressed as

$$L_{d+r}(r) = 10 \cdot \lg\left[\left(I_{d,n} + I_{r,n}\right)/S\right] \qquad (9)$$

where $I_{d,n} = P \cdot Q/(4\pi \cdot r_n^2)$ is the direct sound with power P, directivity Q, $I_{r,n} = 4 \cdot P \cdot (1-\alpha^*)^{r_n/l_n+1}/\alpha^*$ is the reverberant intensity with α^* characteristic sound absorption (including absorption of the medium) and l_n normalized MFPL. Normalization by the $\sqrt{S}$ term is used also in the distance $r_n = r/\sqrt{S}$.
This formulation suggests, that total sound level depends on normalized (relative) distance (r_n) in the room, shape (l_n) and size (S) of the room, energy losses (α^*) in the room, sound power (P) and directivity of the source (Q) and that it requires only the existence of an exponential spatial decay (characteristic MFPL and absorption), not a diffuse field of strict sense.
This model fits experience remarkably, but the concept of MFPL is not valid in the early response, so spatial decay has more to do with how direct illumination of boundaries decrease with distance from the source in the first place. In addition, with non-uniform sound absorption, spherical symmetry becomes distorted and an angle-dependent rate of spatial decay is expected.

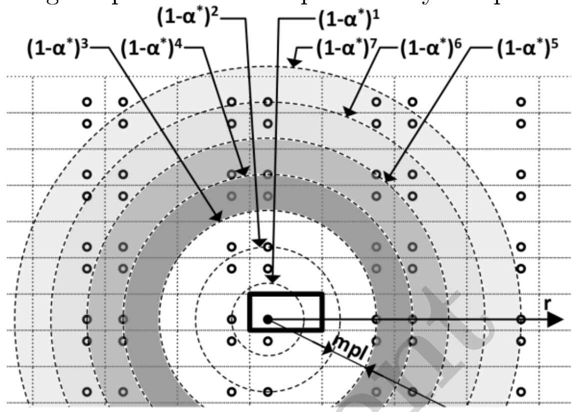

Figure 6. Spatial decay of reflected sound levels can be approximated by extrapolating validity of the concept of MFPL back to near the source.

7. Analysis in the frequency-domain

In order to find limits in the frequency domain, we look at spatial distributions of pure tone responses.
Responses are calculated using MISM and collected along a uniform $\Delta x < \lambda/2$ grid (see Figure 7) in a room. A linear time-invariant room response of a pure tone excitation will be a sum of sinusoid signals of the same frequency. Effects of reflections in the sum are represented by phase-shifts accumulated and attenuations multiplicated.
Stochastic (e.g. diffuse) reflections can be considered by adding phase uncertainty at each reflection. Phase uncertainty has uniform distribution on $[0 \dots 2\pi\delta]$ range at each reflection, where $\delta = 0 \dots 1$ like the diffuse reflection coefficient. A Monte Carlo simulation can then give a robust estimate on this random process. When $\delta = 0$, reflection is added coherently, while a $\delta = 1$ reflection results in incoherent summation.

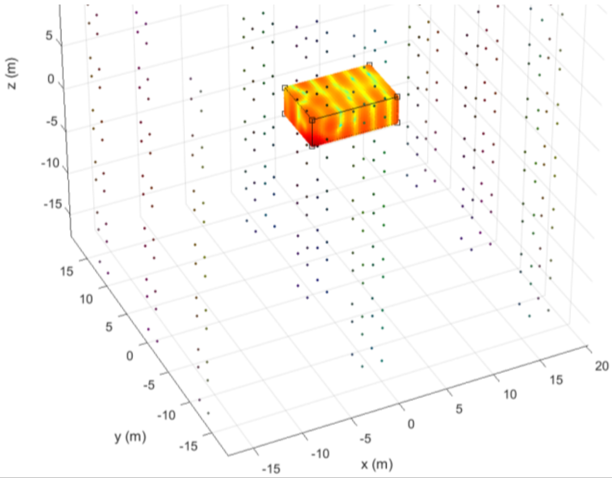

Figure 7. View on a 3D MISM experiment of a 9×6×3 m room, $\Delta x = 0.25$ m receiver mesh, uniform $\alpha = 0.10$

Preliminary document

absorption, $\delta = 0.00$ diffuse reflection, {0.1;0.1;0.1} m source position, 100 Hz frequency.

In Figure 8, filled contour plots of different indicators are shown as a function of frequency and uniform sound absorption coefficients changed from 0.05 to 1.00. Calculation results show, that standard deviation (SD) of sound pressure levels (SPL in dB) or RMS sound pressures do not consistently correlate to ranges, where SA is considered to be valid. Nevertheless, nSD of RMS sound pressure is a more suitable indicator.
It seems practical to plot nSD relative to nSD_{free}, which is the nSD of the direct pure tone field (when $\bar{\alpha}_s \approx 1$) within the given volume. The reasoning can be, that if spatial variability of the field in a room is close to the one in the free-field condition, it can indicate a homogenous (un-biased) reflected field.
On the contour plots different thresholds are shown:

- solid lines: lower frequency limit, modal overlapping is not lower than 3, based on $\Delta f = 2.2/T_{60}$ modal bandwidth, where T_{60} is calculated for each mode (gray, see [16]), or Sabine (black), Eyring (blue) and (8) (red) formulas.
- dotted lines: SF calculated according to (1) colored the same way as for the solid lines.

Please note, that blue ($T_{60,E}$) and red ($T_{60,M}$) thresholds are coincident, when sound absorption is the same on all boundaries (i.e. $\mu = 1$).

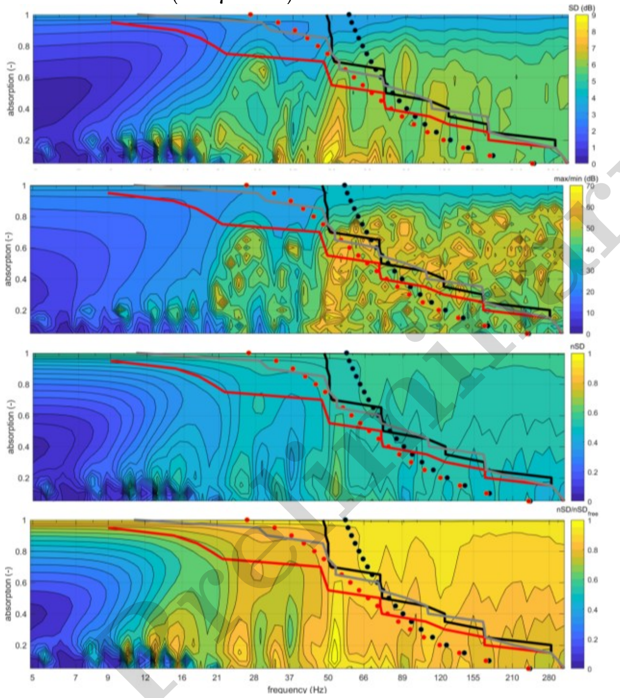

Figure 8. Comparing different indicators based on results of the same case (see Figure 7, absorption is uniform, $\delta = 0.00$, MISM up to 0.4 s). From top: SD of SPL (dB), max/min of sound pressure (dB), nSD then nSD/nSD_{free} of sound pressure. Thresholds (dotted+solid lines) are explained in the description in detail.

Figure 9 shows, how contour plots of nSD/nSD_{free} and threshold change when sound absorption is not uniform. Selected boundaries have 0.99 of sound absorption, while others are changed uniformly from 0.05 to 0.95 in 0.05 steps. Now blue and red thresholds are different and the red ($T_{60,M}$ based) curve seems to follow trends in nSD/nSD_{free} more closely. Limit f_{Sch} (dotted thresholds) seems to be safe, when absorption is higher, but tends to be loose otherwise, when compared to modal counts (solid line thresholds).
Figure 10 shows, how phase uncertainty affects plots of nSD/nSD_{free}. As expected, higher uncertainty makes wave-shape-dependent tendencies to diminish.

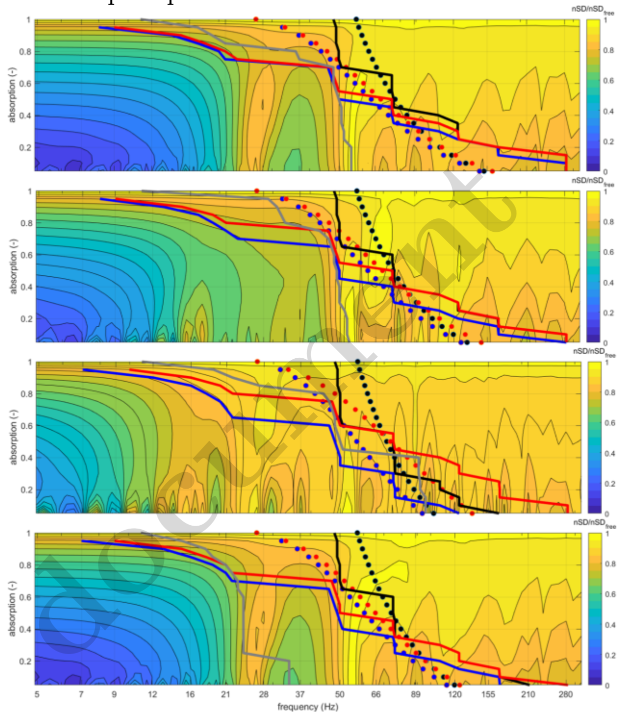

Figure 9. Effect of non-uniform sound absorption on nSD/nSD_{free} plots of the same case (see Figure 7, when $\delta = 0.00$). Except for selected surfaces, sound absorption is uniform. From top: only $\{\alpha_{L,1}\} = 0.99$, only $\{\alpha_{W,1}\} = 0.99$, only $\{\alpha_{H,1}\} = 0.99$, then $\{\alpha_{L,0}; \alpha_{L,1}\} = 0.99$.

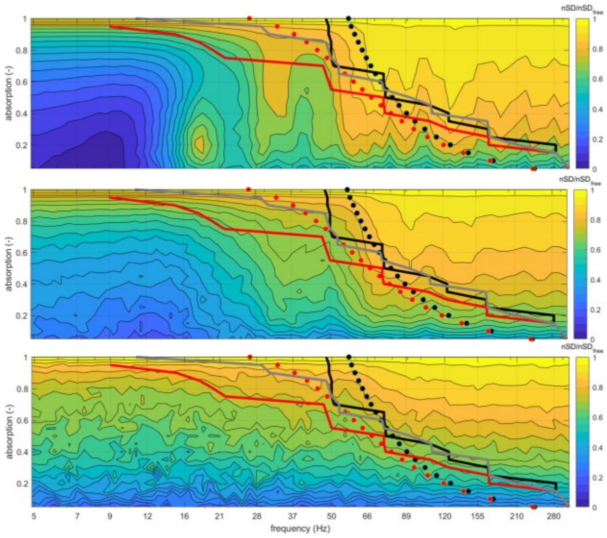

Figure 10. Effect of phase uncertainty sound absorption on nSD/nSD_{free} plots of the same case (see Figure 7, absorption is uniform), Monte-Carlo calculation with 30 trials. From top: $\delta = 0.10$, $\delta = 0.20$, then $\delta = 0.40$.

Preliminary document

8. Summary

Simple statistical approximations are considered to be valid above the Schroeder-frequency in the frequency domain and after the mixing time in the time domain. The aim of the paper is to look for similarly practical indicators, but which consider dimensional proportions of the room and non-uniform sound absorption.
Findings of the paper are derived from results of MISM with an extension to model stochastic reflections using the Monte-Carlo method.
Calculations confirm, that development of isotropy is faster when the room shape is more compact, which correlates to the MFPL-based form factor. This is expressed in an empirical limit t_{iso} from the condition that the normalized standard deviation (or nSD) of directional distribution of reflections is lower than 0.1. This arbitrarily chosen threshold seems to work well, but should be verified and tuned to match experience.
The paper approximates cases with non-uniform sound absorption by introducing 'apparent' sizes of the room. Based on the apparent MFPL, a new reverberation time formula is presented. The apparent form factor can indicate how non-uniform sound absorption changes t_{iso} and indicates validity of classic formulas.
A homogeneous reverberant sound level is traditionally associated with the validity of SA. However, reverberant sound level is known to have a spatial decay in practice, which the concept of MFPL can approximate.
Finally, the paper demonstrates, that nSD of responses to pure tone excitation correlates to regions and tendencies considered to be valid for SA. On the same graphs, frequency-domain limits based on Schroeder-frequency (SF) formula and modal overlapping counts are compared. SF seems to be safe to use, but compared to modal overlapping counts, SF underestimates cross-over frequency limits, when absorption is low.

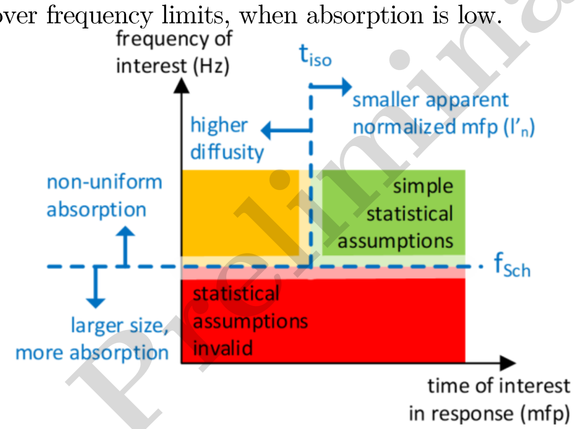

Figure 11. Validity of statistical approximation is a function both of frequency and time within the response, where limits like f_{Sch} and t_{iso} are affected by basic characteristics.

Similar to [5] Figure 13 summarizes the results in how discussed attributes affect validity of statistical assumptions in the frequency and time domain.
Effects of directional scattering was not discussed but surely lower t_{iso}. Experimental validation is necessary to support these findings.

References

[1] M. Schröder, "Die statistischen Parameter der Frequenzkurve von großen Räumen" Acustica 4, pp594–600 (1954)

[2] M. Skålevik, "Schroeder Frequency Revisited", Forum Acusticum 2011, Aalborg, Denmark (2011)

[3] M. R. Schroeder, "The Schroeder frequency revisited", J. Acoustic. Soc. Am. 99 (5) pp3240-3241 (May 1996)

[4] S. Abel, et al., "A Simple, Robust Measure of Reverberation Echo Density", AES 121st convention, San Fransico (October 2006)

[5] J. Tot, L. Cerveau, O. Warusfel, "Analysis and Synthesis of Room Reverberation Based on a Statistical Time-Frequency Model", J. Acoustic. Soc. Am. 99, pp2530-2574 (1996)

[6] M.Nolan, "Experimental characterization of the sound field in a reverberation room", PhD thesis, TU Denmark (2019)

[7] R. Badeau, "Common mathematical framework for stochastic reverberation models", J. Acoustic. Soc. Am. 145, p2733 (2019)

[8] J. B. Allen, D. A. Berkley, "Image method for efficiently simulating small-room acoustics", J. Acoustic. Soc. Am. 66(4) April 1979, pp943-950

[9] J. H. Rindel, "On the Reflection of a Spherical Sound Wave from a Finite Size Surface", Applied Sciences 16 (9):4243 (April 2026)

[10] R. Neubauer, B. Kostek, "Prediction of the Reverberation Time in Rectangular Rooms with Non-Uniformly Distributed Sound Absorption", Archives of Acoustics, Vol. 26 (2001)

[11] A. D. Pierce, "Acoustics: An Introduction to Its Physical Principles and Applications", ISBN 0-88318-612-8

[12] M. Tohyama, A. Suzuki, "Reverberation Time in an Almost-Two-Dimensional Diffuse Field", J. Sound Vib., 111(3), pp391-398 (1980)

[13] A. T. Fürjes, "Comparing Derivation from the Revised Theory of Sound Level Distribution in Rooms to Measurement Results", DAGA 2023

[14] M. Barron, L-J. Lee, "Energy relations in concert auditoriums", 1988, JASA 84(2), pp618-628

[15] L. Nijs, M. Rychtárikova, "Calculating the Optimum Reverberation Time and Absorption Coefficient for Good Speech Intelligibility in Classroom Design Using U50", 2011, Acta Acustica united with Acustica, Vol. 97 (2011) pp93-102

[16] J. H. Rindel, "Modal Energy Analysis of Nearly Rectangular Rooms t Low Frequencies", Acta Acustica, Vol. 101 1211-1221 (2015)

Preliminary document